Demonstration of stripmap mode synthetic aperture ladar with PGA-independent high resolution images

Wu Jin[1], Li Feifei[2], Zhao Zhilong[2], Yang Zhaosheng[2], Wang Donglei[1], Tang Yongxin[1], Su Yuanyuan[2], Liang Na[2]

(1. Institute of Electronics, Chinese Academy of Sciences, Beijing 100190, China;
2. University of Chinese Academy of Sciences, Beijing 100049, China)

Abstract: Synthetic aperture ladar (SAL) has the potential to image long distance objects with high resolutions. However, due to the short laser wavelength used, tiny mechanical vibrations in the SAL system will possibly course enormous phase errors in the target backscattered signals. As a result, it is difficult to obtain stable phase history data in SAL and high resolution SAL images are usually formed by additional phase error removing techniques, especially phase gradient autofocus(PGA) technique. In this paper, a well-performed stripmap mode SAL is demonstrated in the laboratory. Using a linearly wavelength scanning laser in the 1 550 nm range as the detecting source, the SAL can generate well-focused high resolution images. By carefully designing the system, most mechanical vibrations that will introduce phase errors into the backscattered signals are suppressed. The phase history data generated in the SAL are so stable that high resolution images are formed by straightforwardly following the standard SAL image formation theory and not relying on PGA. Using dot target calibration, both the azimuth and range resolutions of the SAL are measured to near its theoretical estimations. At target distance of 2.4 m, well focused SAL images with various targets, together with their stable phase history data, are illustrated in detail.

Key words: SAL; stripmap mode; phase history data
CLC number: TN958 Document code: A Article ID: 1007-2276(2014)11-3559-06

条带模式合成孔径激光雷达不依赖 PGA 的高分辨率成像演示

吴 谨[1],李斐斐[2],赵志龙[2],杨兆省[2],王东蕾[1],唐永新[1],苏园园[2],梁 娜[2]

(1. 中国科学院电子学研究所,北京 100190; 2. 中国科学院大学,北京 100049)

摘 要: 合成孔径激光雷达(SAL)能实现远距离目标的高分辨率成像。然而,由于所用激光波长很短,SAL 系统中微小机械振动都可能在目标回波信号中引入巨大相位误差, 所以,SAL 很难实现稳定的相位史数据,高分辨率 SAL 图像的形成往往要应用额外的相位误差消除技术,特别是相位梯度自聚焦(PGA)技术。演示了一个运转良好的条带模式 SAL 实验室成像装置。采用一台 1 550 nm 波段的线性

收稿日期:2014-03-11; **修订日期:**2014-04-10
基金项目:国家自然科学基金(61178071);国家 863 计划(2007AA12Z107)
作者简介:吴谨(1965-),男,研究员,博士生导师,博士,主要从事合成孔径激光雷达成像技术方面的研究。Email:jwu909@263.net

调波长激光器作为探测光源,该装置能够形成聚焦良好的高分辨率图像。通过细致的系统设计,基本抑制了在回波信号中产生相位误差的各种振动。该装置产生的相位史数据非常稳定,高分辨率图像的形成仅需简单遵照标准的 SAL 成像理论,无需额外借助 PGA。采用点目标定标,测量得到该成像装置的方位和距离分辨率接近其理论估计。详细给出了 2.4 m 距离上多种目标的良好聚焦图像及相应的稳定相位史数据。

关键词:合成孔径激光雷达; 条带模式; 相位史数据

0 Introduction

The research on synthetic aperture ladar (SAL) can be dated back to 1970s[1-2]. These early efforts, together with those later finished by C. C. Aleksoff, et al. with a TEA CO_2 laser in 1987[3] and by Stephen Marcus, et al. with a solid state laser in 1994[4], were further advanced by M. Bashkansky, et al. in 2002[5] and by S. M. Beck, et al in 2004[6], where M. Bashkansky, et al. demonstrated the first two-dimensional SAL image in the optical domain and S. M. Beck, et al. obtained the first SAL image of a diffusive target. Following these achievements, outdoor SAL experiment and SAL flight test are also reported[7-8].

SAL is fundamentally a coherent technique that relies on the phase history data (PHD) from pulse to pulse to achieve high resolution in the cross-range dimension[9]. Due to the short optical wavelength used, it is rather difficult to maintain stable PHD during the synthetic aperture time. As a result, among the reports released on SAL development, whether laboratory demonstrations[6] or flight test[8], the high resolution SAL images are usually focused by the aid of phase error correcting algorithms as phase gradient autofocus (PGA)[9]. Typical SAL performance showing PGA-free images of high resolution obtained by stable PHD is rarely disclosed.

In this article, we demonstrate a stripmap mode SAL imaging system in laboratory that can generate stable PHD and thus form high resolution images by simply following the standard image formation theory and not using PGA. Detailed results showing vivid focusing steps on dot or extended targets are illustrated.

1 Experimental setup

The experimental setup is shown in Fig.1. The linear polarized laser light from the laser source (Anritsu: Tunics Plus tunable laser) is first 90/10 split by 1×2 PM fiber coupler OC1. The 90% part is used as the detecting light, which is first collimated by fiber collimator L1, then passed through inverted 10X telescope BE1 to form a diverged laser beam of waist size about 0.5 mm in diameter and 3.3 mrad in full divergence angle. This divergent beam is circular polarized by an optical isolator (composed of polarization beam splitter PBS and quarter wave-plate QW in Fig.1) before illuminating the target. The other 10% part from OC1 is again 90/10 split by 1×2 PM fiber coupler OC2, where the 90% portion is further equally split by 1×2 PM fiber coupler OC3 and the rest 10% portion is made travel through fiber collimator L3, molecular gas cell HCN (Thorlabs: CQ09075-HCN13) and fiber collimator L4 so as to be recorded by photodiode D3. As to the laser beam from OC3, one half is acted as the local light required by heterodyne detection with the scattered light from the target and the other half is again equally split by 1×2 PM fiber coupler OC4 to form the reference channel heterodyne signal used by sharpness technique in raw data matrix formation [9-10]. OC5 and OC6 are two 3 dB 2×2 PM fiber couplers required by the balanced detectors D1 and D2, respectively. Three amplifiers A1, A2 and A3 are used to properly amplify electrical signals from D1, D2 and D3, respectively so as to suit for digitalization.

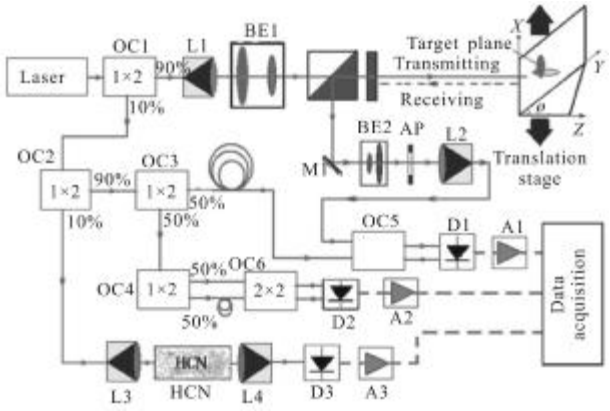

Fig.1 Experimental setup for stripmap mode SAL imaging demonstration

In the receiving signal channel, 10X beam expander BE2 is used to enlarge the receiving field of view (FOV) limited by the fiber collimator L2 and the fiber core. Moreover, a rectangular aperture AP is placed behind BE2, forming an equivalent receiving aperture of about 0.5 mm×0.5 mm.

The target plane **XY**, with a tilt angle ϕ to the laser propagation direction in **Z** axis, is mounted on a translational stage that can be moved across the laser beam in azimuth direction **X**. By varying the tilt angle ϕ of the target plane, different SAL setups can be simulated, for example, ϕ=45° corresponds to a side-looking SAL, ϕ=90° to a down-looking SAL, etc.

The SAL setup in Fig.1 is actually a similar version to that in Ref.[5-6]. Three signal channels are setup: channel with D1 is the signal channel recording the target scattered light by heterodyne detection, channel with D2 is the reference channel recording the nonlinear chirp induced by the wavelength scanning of the laser source and channel with D3 is the absorption channel recording the baseline frequency labeled by the molecular gas cell HCN. Data acquisition of these three channels is realized by a four-channel oscilloscope (Lecroy: Wavesurfer 44Xs) with 8 bit A/D converters.

To avoid possible disturbance to PHD, most of the optical components in the SAL setup are placed on a vibration-isolated optical stage. Other apparatus and electronic devices are also carefully allocated.

During data acquisition, the SAL performs in "start-stop" mode: the target holds still while the laser is chirped from 1 530 nm to 1 570 nm with a wavelength scanning speed of 100 nm/s and the target is moved to the next azimuth sampling position with constant speed after the laser chirping and data acquisition are both finished.

Experimental parameters of the SAL setup are listed in Tab.1.

Tab.1 Parameters of SAL setup

Item	Parameter	Value
1	Laser power/mW	5.0
2	Wavelength scanning speed/nm·s^{-1}	100
3	Pulse length/ms	100
4	Target distance/m	2.4
5	Synthetic aperture length/mm	8
6	Azimuth step length/μm	50
7	Equivalent receiving aperture/mm×mm	0.5×0.5
8	SAL imaging mode	Stripmap

Raw data matrix for SAL imaging is generated by the methods provided in Ref.[6], such as using the absorption channel data to synchronize the baseline frequency, using reference channel data to remove the nonlinear chirp error by sharpness technique, etc. And, as listed Tab. 1, despite that the laser source is wavelength scanned from 1530 nm to 1570 nm in a period of 400 ms, only the middle part of 100 ms is used as the chirping pulse-length to form SAL image.

The image are generated by following the standard image formation theory on SAL[11]: the range compressed image is obtained by Fourier transformation to the raw data matrix in the range direction and the final SAL image is focused by matched filtering the range compressed data in the azimuth direction.

The matched filter used for azimuth focusing in the SAL setup is expressed in the following simple form.

$$\mathbf{h}(x_m)=\exp\left[-j2\pi f_0\left(\frac{x_m^2}{cL_0}\right)\right] \quad (1)$$

Where x_m, f_0, c and L_0 are the azimuth sampling position, baseline frequency of the transmitting light, speed of light and target distance, respectively.

Using data in Tab.1 and Eq.(1), the theoretical estimation of the resolutions on the imaging plane in side-looking SAL configuration can be calculated out as follows:azimuth resolution: $\delta x \approx 230\ \mu m$, range resolution: $\delta y \approx 170\ \mu m$.

2 Experimental results

2.1 Single dot target

A target composed of a single dot is used to observe the performance of the SAL setup, which is made of a silver coated plane mirror covered by a piece of black paper with only a small hole of about 350 μm in diameter. The plane mirror is carefully adjusted to perpendicular to the axis of the transmitting light. In this case, ϕ=90° and the SAL image will occupy one range element only.

Fig.2 is the result with this dot target. Fig.2(a) is the amplitude distribution of the raw SAL data. Fig.2(b) and 2(c), obtained by following standard SAL image formation theory, are the amplitude distributions of the range compressed image and aperture synthesized image, respectively. Fig.2 (d) shows the azimuth PHD of the range compressed data, which is a well-shaped quadratic profile. From Fig.2 (a) to (c), a typical two-step focusing process is displayed.

Both the azimuth and range resolutions of this SAL setup can be estimated using the data in Fig.2(d). Fig.2(e) and 2(f) show the details of the intensity distributions of Fig.2(d) in range and azimuth direction, respectively. The full width half maximum(FWHM) of Fig.2(e) is about one range element, just the theoretical prediction. And the FWHM of Fig.2(f) is about 7 azimuth steps or 7×50 μm =350 μm, which is closed to the theoretical value of 230 μm.

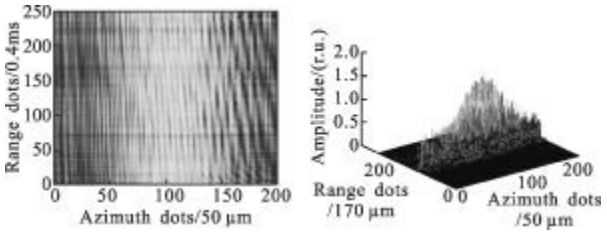

(a) Raw data (amplitude) (b) Range compressed image (amplitude)

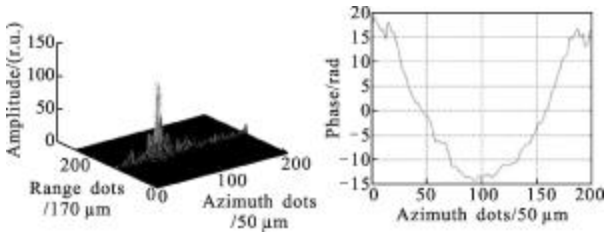

(c) Azimuth focused image (amplitude) (d) Azimuth phase distribution of Fig.2(c)

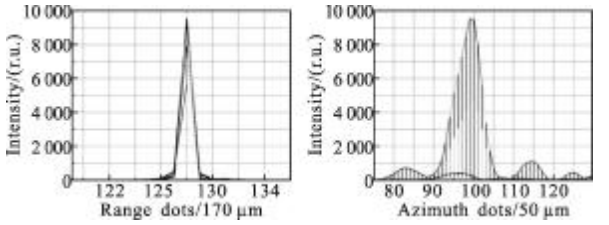

(e) Range intensity distribution of SAL image (f) Azimuth intensity distribution of SAL image

Fig.2 SAL image of a dot target

2.2 Doted targets or extended targets

Fig.3 gives the result of a two-dot target lined in azimuth direction under ϕ=90°. Fig.3(a) is the raw data showing interference fringes. Fig.3(b) and Fig.3(c) are the amplitude distributions of range compressed image and final aperture synthesized image, respectively. Fig.3(d) shows the quadratic azimuth phase distribution

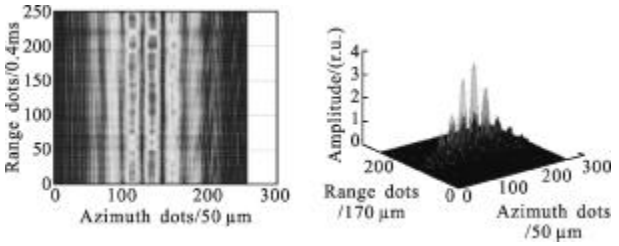

(a) Raw data(amplitude) (b) Range compressed image (amplitude)

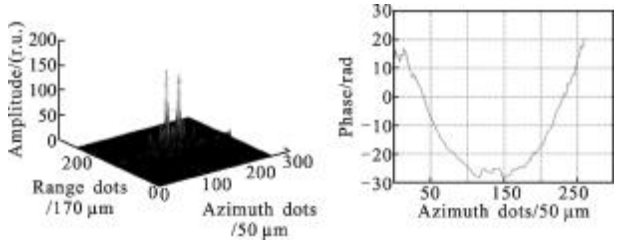

(c) Azimuth focused image (amplitude) (d) Azimuth phase distribution of Fig.3(b)

Fig.3 SAL image of an azimuth lined two-dot target

of the range compressed SAL data in Fig.3(b). Again, a quadratic PHD profile is obtained in Fig.3(d).

Fig.4 gives the result on an extended target made of "3M" diamond retro-reflective material under $\phi = 45°$. This configuration is usually referred to as side-looking in SAL terminology. The target, shown in Fig.4(a), is five letters "IECAS" with size of about 50 mm(azimuth)×8 mm(range). Fig.4(b) is the raw data showing the "chaotic" interference pattern. Fig.4(c) and 4(d) are the amplitude distributions of the range compressed image and azimuth synthesized image, respectively. In Fig.4(c), there are strong bright lines near No.100 range element and the five letters are hardly discriminated; however, after matched filtering, the strong bright lines disappear and five letters clearly emerge in Fig.4(d). From Fig.4(b) to (d), again, a two-step focusing process is displayed. Fig.4(e) shows the azimuth PHD of range element No.127 in Fig.4(c).

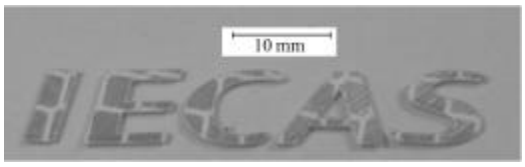

(a) Photograph of target

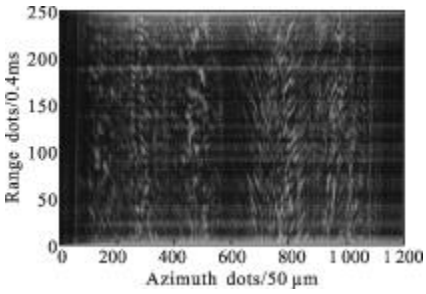

(b) Raw data(amplitude)

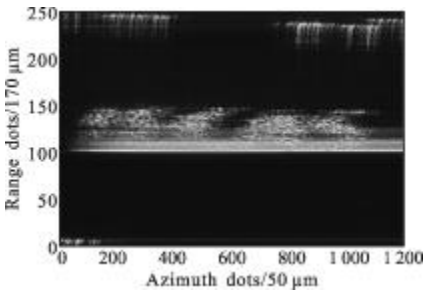

(c) Range compressed image(amplitude)

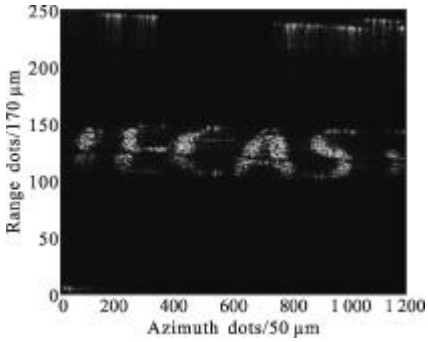

(d) Azimuth focused image (amplitude)

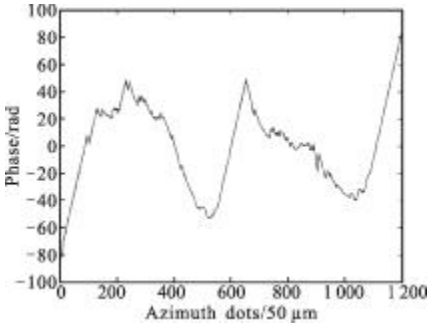

(e) Azimuth phase distribution of range element No.127 in Fig.4(c)

Fig.4 SAL images of letters "IECAS"

Figure 5 shows a big SAL image in side-looking configuration. Fig.5(a) is the photograph of the target, which is the logo of the Institute of Electronics, Chinese Academy of Sciences. The logo, stuck on a

(a) Photograph of target

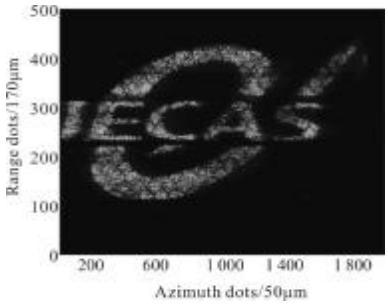

(b) Focused SAL image

Fig.5 Mosaic SAL image of a logo pattern

black rubber plate, is also made of "3M" diamond retro-reflective material by laser cutting. The overall extending size is about 100 mm (azimuth)× 68 mm (range). Due to the limited receiving FOV in this SAL setup, altogether nine vertical scans have been carried out in order to cover the whole pattern. Fig.5(b) is the final SAL image joined by the nine scans. The SAL image is well-focused, clearly showing the surface details.

3 Conclusion

A stripmap mode SAL in the laboratory is demonstrated, which can achieve stable PHD and generate well-focused images by following the standard SAL imaging formation theory and not relying on PGA. At a target distance of about 2.4 m, the SAL generates images on various targets with azimuth resolution of no more than 350 μm and range resolution of about 170 μm. Detailed imaging results on dot or extended targets straightforwardly show the typical performance of SAL.

Moreover, all devices and components used in the SAL setup are commercially available. Stable PHD is achieved not by using a laser with superior phase stability but by carefully overcoming the obstacles that may cause phase disturbance. The results show that, despite the short laser wavelength used in SAL, it is workable to build a SAL imaging system, at least in the laboratory, that agrees well with theoretical prediction and does not require PGA to focus images.

Acknowledgments

We greatly appreciate the support from Prof. Yirong Wu, Academician in Chinese Academy of Sciences, as well as the valuable discussions on SAR signal processing by Prof. Chang Liu in the Institute of Electronics, Chinese Academy of Sciences.

References:

[1] Lewis T S, Hutchins H S. A synthetic aperture at optical frequencies[C]//IEEE, 1970, 58(4): 587-588.

[2] Lewis T S, Hutchins H S. A synthetic aperture at 10.6 microns[C]//IEEE, 1970, 58(10): 1781-1782.

[3] Aleksoff C C, Accetta J S, Tai L M, et al. Synthetic aperture imaging with a pulsed CO_2 TEA laser [C]//SPIE, 1987, 783: 29-40.

[4] Marcus S, Colella B D, Green T J J. Solid-state laser synthetic aperture radar[J]. Appl Opt, 1994, 33(6): 960-964.

[5] Bashkansky M, Lucke R L, et al. Two-dimensional synthetic aperture imaging in the optical domain [J]. Opt Lett, 2002, 27(22): 1983-1985.

[6] Beck S M, Buck J R, Buell W F, et al. Synthetic aperture imaging ladar: laboratory demonstration and signal processing [J]. Appl Opt, 2005, 44(35): 7621-7629.

[7] Buck J R, Krause B W, Malm A I R, et al. Synthetic aperture imaging at optical wavelengths [C]//Conference on Lasers and Electro-Optics (CLEO), 2009: PThB3.

[8] Krause B W, Buck J, Ryan C M, et al. Synthetic aperture ladar flight demonstration [C]//Conference on Lasers and Electro-Optics (CLEO): Applications and Technology (CLEO_AT), 2011: PDPB7.

[9] Ricklin J C, Tomlinson P G. Active imaging at DARPA[C]// SPIE, 2005, 5895: 589505.

[10] Eichel P H, Wahl D E, Ghiglia D C, et al. Phase gradient autofocus -a robust tool for high resolution SAR phase correction [J]. IEEE Trans on Aerospace and Electronic System, 1994, 30(3): 827-835.

[11] Wu Jin. Matched filter in synthetic aperture ladar imaging[J]. Acta Optica Sinica, 2010, 30(7): 2123-2129. (in Chinese)
吴谨. 合成孔径激光雷达成像之匹配滤波器 [J]. 光学学报, 2010, 30(7): 2123-2129.